CONF 890903--2

HADRON COLLIDER PHYSICS AT FERMILAB

ANL-HEP-CP--89-122

DE90 003384

Lawrence J. NODULMAN

High Energy Physics Division, Argonne National Laboratory, Argonne, Illinois 60439 USA

The hadron collider physics program at Fermilab, Tevatron-I, has recently provided considerable data samples to two high beta experiments as well as one low beta general purpose Collider Detector at Fermilab (CDF). A brief description of the Tevatron collider and the high beta experiments is followed by a discussion of hard scattering results from CDF. The prospects for growth in this exciting physics program are outlined.

1. INTRODUCTION: THE TEVATRON COLLIDER

The four mile superconducting accelerator ring at Fermilab, the Tevatron, has been turned into a quite productive proton-antiproton collider. The process starts with a linac and booster to provide 8 GeV protons. The main tunnel houses both the Tevatron and the conventional main ring. The main ring accelerates protons and antiprotons for injection into the Tevatron as well as accelerating protons to target for creating antiprotons. The antiprotons get a first dose of cooling and bunch rotation in the debuncher ring before transfer to the accumulator ring. Once a sufficient density of antiprotons has been achieved, slices of phase space are removed from the accumulator into the main ring. The main ring performs RF manipulations to form individual dense bunches which are deposited in the Tevatron at 150 GeV. Six bunches of each are accelerated to 900 GeV, brought into collision at the nominal places, squeezed at B∅ (CDF), and scraped to reduce backgrounds. A basic layout of the Tevatron is shown in Fig. 1 for an upgrade involving removing the main ring and replacing it with a main injector in a separate tunnel. At B∅, the main ring makes a vertical bypass above the CDF detector where it is effectively shielded by two feet of steel complemented by anticoincidence counters.
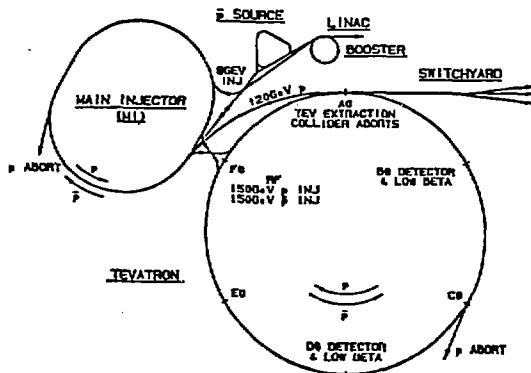

FIGURE 1
Layout of the Fermilab Tevatron. In this version, the main ring has been replaced by a proposed Main Injector in a separate tunnel.

First collisions were observed in TeV-I by a partial CDF detector in October 1985. In the spring of 1987, the first physics run provided small data samples to CDF and the high beta experiments. We have recently completed (end of May, 1989) a one year collider run which greatly exceeded even our most optimistic projections. Typical starting luminosities were $1.7 \times 10^{30}/$ cm^2/sec with lifetime growing from 12 to 24 hours. More than 9 pb^{-1} was produced at B∅ of which CDF captured about half with a very broad set of triggers and fully functional essential detectors. Various special runs at different energies etc. were quite readily performed. In

fact the accelerator staff at Fermilab did a fantastic job of making things work well and keeping them going.

2. HIGH BETA EXPERIMENTS

Two experiments have been running at high beta collision areas of the Tevatron at E0 and C0. The E0 experiment (710) is a Roman pot elastic scattering etc. experiment, while the C0 experiment (735) uses multiplicity counters and a spectrometer to look for quark gluon plasma effects.

The E0 experiment (710) is a collaboration from Bologna, Cornell, Fermilab, George Mason, Maryland, and Northwestern. The basic idea is to measure the total cross section, dσ/dt into the Coulomb interference region to get the ρ parameter, and to study diffraction. There are two Roman Pot stations on either side of E0, the outer pots at effectively 80m. The covered range is $0.0007 < |t| < 0.7$, and data has been obtained at CM energies of 0.3, 0.546, 1.0 and 1.8 TeV. In a preliminary analysis at 1.8 TeV, they have obtained an elastic slope of $B = 16.3 \pm 0.5$ GeV^{-2}, which using accelerator luminosity (± 15%) gives the total cross section of about 78 mb, consistent with $\log^2(s)$.[1] A wealth of data on cross section, phases and such should be forthcoming, providing basic understanding of $\bar{p}p$ collisions.

The C0 experiment (735) is a collaboration from Duke, Fermilab, Iowa State, Notre Dame, Purdue and Wisconsin. An arm of magnetic spectrometer with time-of-flight is complemented by barrel and end multiplicity hodoscopes. Their most notable result is the correlation of average p_T with event multiplicity, shown in Fig. 2 for their 0.3 nb^{-1} sample from 1987.[2] The recent run has given them 25 nb^{-1} at 1.8 TeV as well as 0.03 nb^{-1} at 0.3, 0.546 and 1.0 TeV. They have an unique ability to study identified particle p_T distributions down to quite low p_T.
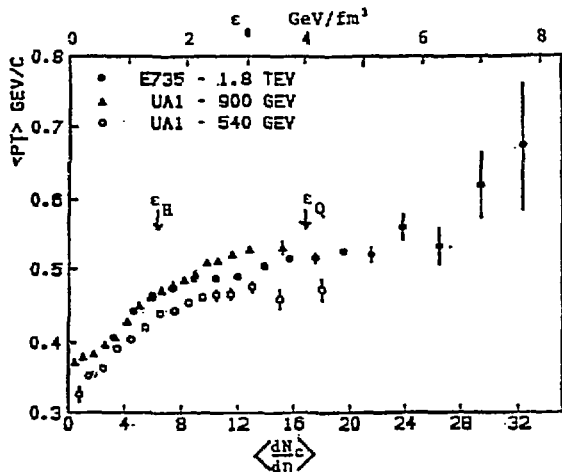

FIGURE 2
Average P_t versus multiplicity. This behavior[2] could have interpretations in terms of quark gluon plasma phase transitions.

3. CDF: DETECTOR, TRIGGER AND DATA

The CDF Group is a collaboration from Argonne, Brandeis, Chicago, Fermilab, Frascati, Harvard, Illinois, KEK, LBL, Pennsylvania, Pisa, Purdue, Rockefeller, Rutgers, Texas A&M, Tsukuba, Tufts and Wisconsin. The detector is designed to be a general purpose search for new physics by detecting and measuring leptons and jets. The CDF detector[3] is shown in Fig. 3.
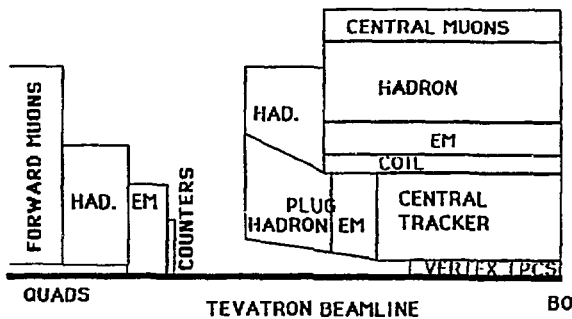

FIGURE 3
Quarter cross section of CDF.

The CDF electromagnetic (EM) and hadron calorimeters have projective geometry similar to that of UA2. Inside of pseudorapidity $|\eta| = 1.2$ the

calorimeters use scintillator, outside gas sampling. The calorimeter surrounds a large superconducting solenoid which produces a 1.4m radius 1.4 Tesla uniform tracking volume. Momentum measurement is provided by an 84 sample tilted jet cell central tracking chamber (CTC) which includes small angle stereo and has good momentum measurement to $|\eta| \approx 1.2$. The CTC surrounds a series of longitudinal drifting TPCs which provide vertex reconstruction and track information to $|\eta| = 3.5$. Drift chambers for muon identification are mounted on the back of the central calorimeter modules and around iron toroids behind the 2-10° setback calorimeter stations. Scintillation counter hodoscopes for triggering are mounted on the inside faces of these calorimeter stations.

The CDF trigger involved four levels. Because the basic calorimeter trigger cycle could not quite keep up with the 3.5 μs cycle between crossings, an East-West hodoscope coincidence (level 0) tagged crossings with interactions, blanking the next crossing. This became a noticeable source of dead time (~ 15%) for the unexpectedly high luminosity! Within 7 μs, the Level 1 trigger took in fast calorimeter signals and formed various sums. The basic electromagnetic trigger was that the sum of EM trigger towers ($\Delta\eta = .2 \times \Delta\phi$ (azimuth) = 15°) individually above 4 GeV exceed 6 GeV. The basic Level 1 jet trigger was that the sum of any trigger towers above 1 GeV exceed 18 GeV. Hardware reconstruction of muon chamber stubs could also produce a Level 1 trigger, which in effect paused the electronics.

The triggers at Levels 2 and 3 formed a long list of permutations and combinations of requirements on clusters of calorimeter energy and tracks. Level 2 used hardware for clustering and tracks to decide if the event should be read out. Level 3 used software running on a farm of ACP 68020 boards in VME to decide if the event should be written out. The triggers which

are relevant to the results to be presented are as follows: 1) a jet trigger requiring a calorimeter cluster above 60 GeV, or 40 or 20 separately prescaled, 2) a central electron requiring a predominantly EM cluster above 12.5 GeV, or 7 GeV prescaled, matched by a hardware found track, 3) a central muon trigger requiring a muon stub matched to a hardware track of at least 9 GeV/c, 4) a photon trigger requiring a predominantly EM cluster above 23 GeV or 10 GeV prescaled, 5) a diphoton trigger requiring two or more predominantly EM clusters above 10 GeV, and 6) a missing E_T trigger requiring at least 25 GeV net transverse energy. Near peak luminosity, events were written out at about 1 Hz.

In 1987, with a much simpler trigger, CDF collected a usable data sample of about 25 nb^{-1}. In the recent run the good/nominal trigger sample is about 4.7 pb^{-1}. This increment makes stringent new requirements for understanding systematics while providing sufficient data for their study.

4. CDF CALIBRATION

With the large sample of collision data available, calibration using data has largely supplanted extrapolation from test beams. The basic idea is to understand the magnetic spectrometer and carry the momentum scale to the calorimeters.

The central tracking chamber alignment began online. Due to the tilted jet cell geometry, each track is a measure of t0 and the drift time relation. Minimum bias events were processed, eventually in real time, to give parameters yielding rms residuals of 160 μ. Overall distortions, which could come, for example, from end plate distortion under tension, fall into two classes – azimuthal alignment which effects resolution at high momentum, and overall magnification which is equivalent to an error in field strength. A sample of 1000 extremely clean central electrons from W → eν has been

used for systematic studies, as Bhabha electrons are used in e^+e^- detectors. By comparing electrons with positrons as a function of polar angle and azimuth, comparing to calorimetry and requiring a (run dependent) common origin, overall azimuthal offsets for each of the 84 depths at each end are determined and the effect of gravity confirmed. This alignment is checked using cosmic rays, where each event provides a positive and negative track which should have the same momentum and extrapolate together. Beam constrained resolution is $0.11\% \times P_t$ after alignment.

The nominal magnetic field as mapped and measured should be known ± 0.05% but since overall distortions can effect the scale, we use the well measured ψ and τ masses to confirm our scale, using $\mu^+\mu^-$ decays in CDF data. The mass distributions are shown in Fig. 4. The ψ agrees perfectly with 0.03% error and the τ is 0.1% high with 0.1% error. We conservatively assign a systematic error of 0.2% to our momentum scale. Note the indication of an τ'.

All CDF calorimeters have online settings based on extrapolations of test beam results using various source systems. The data calibration procedures are accomplished much more readily because these settings proved to be close to final values. For the central EM calorimeter, energy-momentum matching has been used for calibration. For cell-to-cell relative calibration, a sample of 17000 inclusive electrons allows a relative determination of each cell to ± 1.7%, which is then the dominant constant resolution. The absolute scale is set by matching the 1000 clean electron sample, as shown in Fig. 5. The statistical accuracy of the match and the systematic uncertainty in bremsstrahlung corrections increase the ± 0.2% momentum scale to ± 0.4% absolute central EM energy scale.

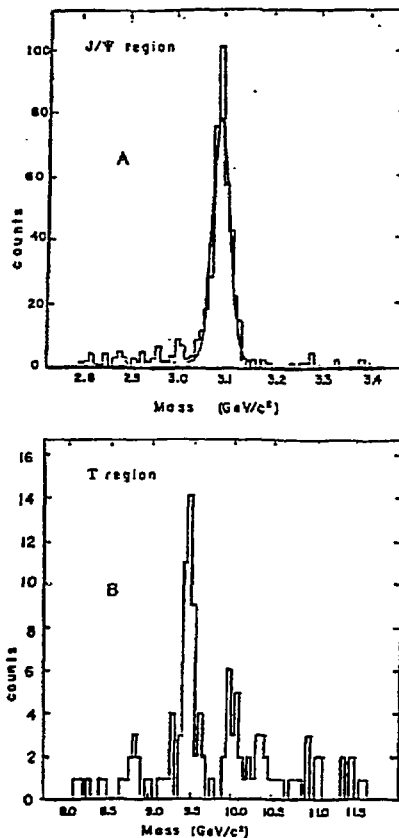For the gas EM calorimeters, accurate momentum is not available. A combination of test

FIGURE 4
Dimuon unlike sign mass distributions in a) the ψ region and   b) the τ region.
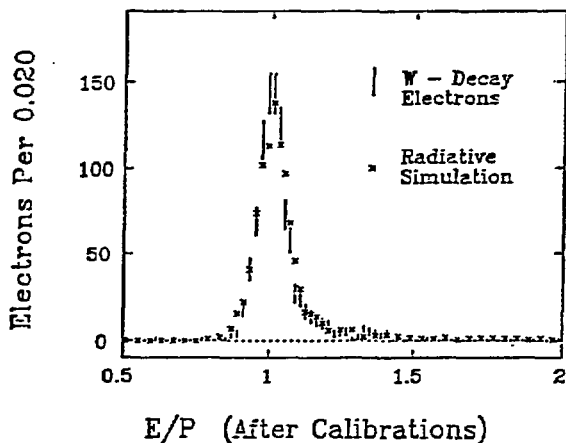

E/P (After Calibrations)

FIGURE 5
Alignment of the 1000 W decay electrons to the radiative Monte Carlo.

beam extrapolation, constraining appropriate candidate $e^{\pm}$ pairs to the Z mass and setting the average electron E_T in W candidates is used to set absolute and quadrant gains. These are further checked in jet balance studies. The gas EM calorimeters are thus not appropriate for determination of the W and Z masses.

For the hadron calorimeters the scale problem is complicated in that the CDF calorimeters are not compensating and there are large nonlinearities which must be taken into account in dealing with jets. Jets in CDF start as clusters - calorimeter energy in cells in a cone of radius 0.7 in $\Delta\eta$, $\Delta\phi$. The nonlinearity has been measured using test beam data and an analysis of isolated tracks in minimum bias events, shown in Fig. 6. This nonlinearity is used with an

FIGURE 6
Nonlinearity of the CDF central calorimeter.

iterated model for fragmentation to obtain jet energy corrections which also account for the finite cone size and background event. These corrections can be checked against the central electromagnetic calorimeter scale by studying E_t balance for events with isolated photon candidates. This procedure needs to be complemented by balance studies of the prolific dijet events in order to be sure that the boundary regions are well understood and simulated. The resulting η dependence is also included in the jet

correction. The average jet correction and its uncertainty is shown in Fig. 7. The extension of the nonlinearity to corrections to lower E_t is also a matter of some concern.
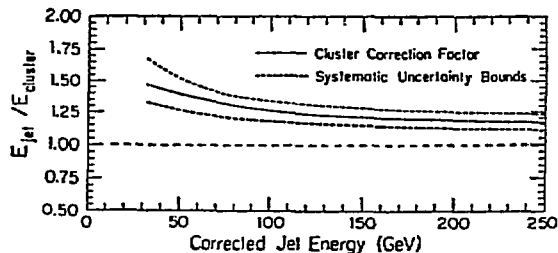
FIGURE 7
Correction factor to go from clusters to jets.

5. CDF JET STUDIES

The E_t distribution of inclusive jets in the central calorimeter has been published from the 1987 data[4] allowing a limit on compositeness[5] of $\Lambda > 700$ GeV. The E_t distribution for 0.9 pb^{-1} of more recent data is shown in Fig. 8. Note
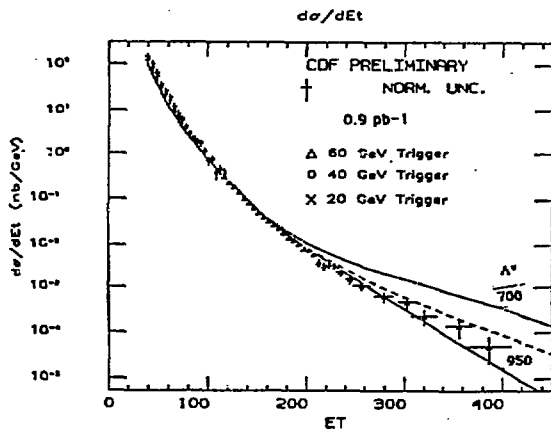
FIGURE 8
Preliminary jet E_t distribution from 0.9 pb^{-1}.

the trigger regions and the reasonable agreement with QCD predictions over nine decades. A preliminary limit $\Lambda > 950$ at 95% CL has been obtained. The nearly complete jet sample is shown for dijet mass in Fig. 9 along with a range of QCD predictions. In principle, the scaled jet cross section can be used to demon-
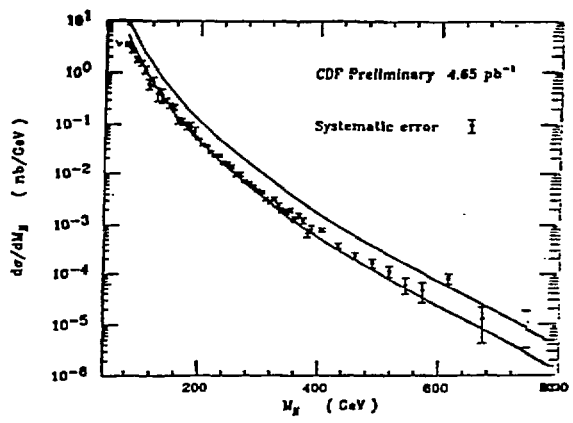
FIGURE 9

Preliminary dijet mass for 4.6 pb^{-1}.

strate the QCD scale breaking effects but the normalization uncertainties of each experiment in the high energy data remove much of the significance. In a special run CDF obtained 10 nb^{-1} of jet data at 0.54 TeV in order to make the measurement with relatively well understood normalization, and this analysis is being actively pursued.
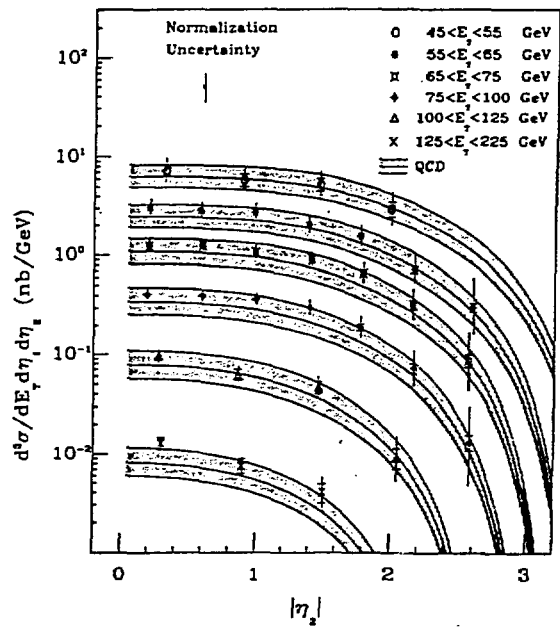

FIGURE 10

CDF 1987 eta distribution for the second jet given a first central jet ($|\eta| < .6$) for ranges of E_t. The bands are a range of QCD calculations.[6]

The angular distributions of two jet events in the 1987 data has been rather thoroughly studied.[6] The polar angle distribution reflects the QCD modification to Rutherford scattering. Another way of understanding this data is shown in Fig. 10; given one jet with $|\eta| < 0.6$, the distribution in $|\eta|$ of the second jet is shown for ranges of E_t along with a range of QCD predictions, as usual lowest order $2 \to 2$ with the range from structure function and Q^2 scale variation.

Three jet angular distributions in the new data are under active study as shown in Fig. 11. The Dalitz plot projections for the leading and second jets are well reproduced by simulation starting from PAPAGENO.[7]
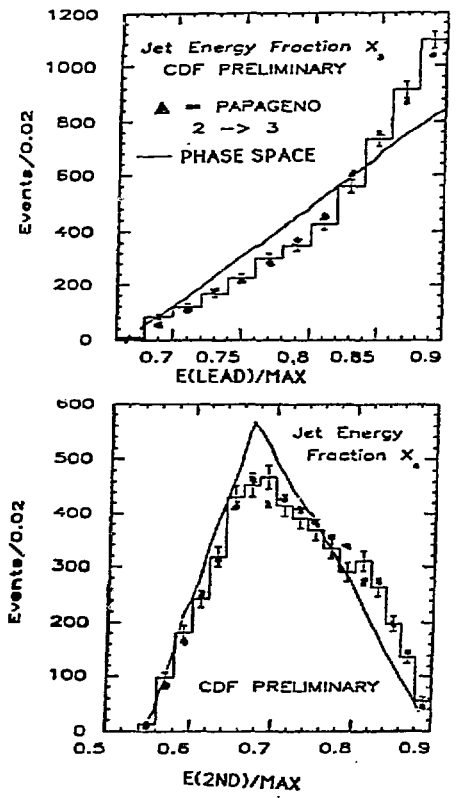

FIGURE 11

Preliminary three jet Dalitz plot projections for a) leading and b) next to leading jets with phase space and PAPAGENO[7] predictions.

Fragmentation of jets has been well studied in 1987 data. The charged fragmentation function is compared to the UA1 measurement[8] in Fig. 12. The integral of that distribution yields an
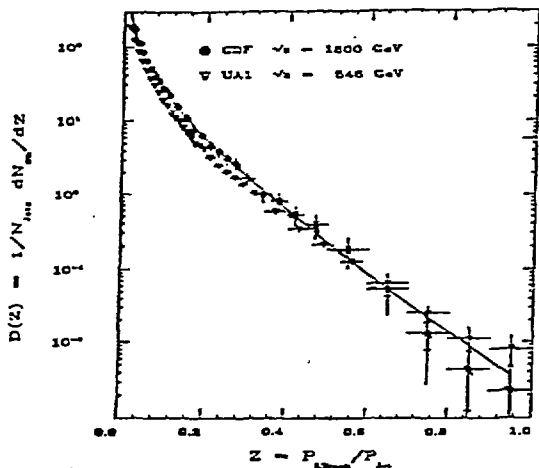

FIGURE 12
CDF preliminary fragmentation function, compared to UA1[8].

average charged momentum fraction of 62 ± 7%, similar to TASSO measurements.[9] Fragmentation functions like structure functions, evolve in QCD as illustrated in Fig. 13. Note that the
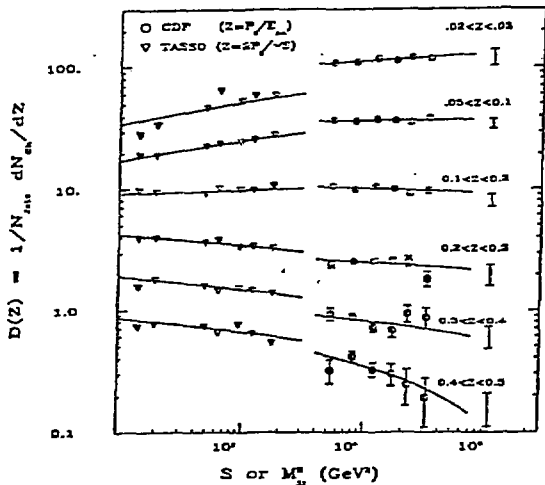

FIGURE 13
Evolution of fragmentation from TASSO[9] and preliminary CDF data.

TASSO data[9] involves mainly quark jets while the CDF data involves mainly gluon jets. The rate of charm pair production in gluon jets can be measured by the extra constraint of the D^*/D mass difference as shown in Fig. 14. The indicated charm fraction for jets of about 46 GeV is 0.10 ± 0.03 in reasonable agreements with expectations as well as indications from UA1.[10]
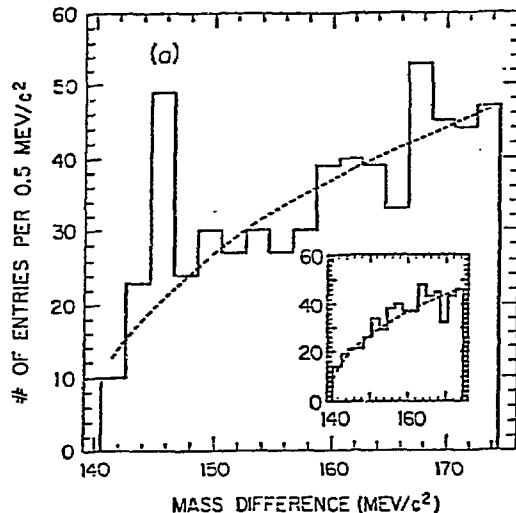

FIGURE 14
D^* signal from 1987 CDF data. Inset shows wrong sign distribution.

We have seen that jet events are well described by QCD in many aspects. Unbalanced jet events can be used to search for new physics such as SUSY. Events are selected with transverse energy imbalance (E_t) greater than 40 GeV. To reduce measurement fluctuation background, the ratio of E_t to the square root of total E_t must be above 2.8. At least two clusters are required in the region $|\eta| < 3.5$ with cluster E_t > 15 GeV and 10-90% EM energy. At least one cluster E_t > 15 must be central ($|\eta| < 1$) and have matched charged tracks corresponding to at least 20% of its E_t. Dijet topologies are removed by requiring that there be no cluster above 5 GeV within ± 30° in azimuth of being opposite to the leading cluster. To reduce

backgrounds from cosmic rays and W decays, a cluster above 15 GeV with > 90% EM energy, a central muon candidate with p_T > 15 or passive muon candidate (track p_T > 15, calorimeter consistent with minimum ionizing, $|\eta|$ < 1.2) cause events to be rejected. An additional 18 events are removed on inspection as being due to noise, cosmic rays, readout errors or beam gas interactions, leaving the 184 events shown in Fig. 15.
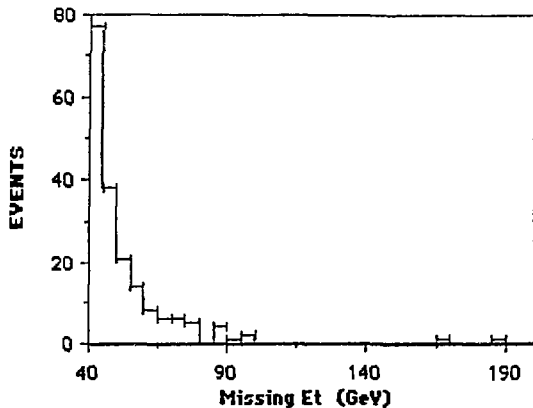

FIGURE 15
Missing E_t for the preliminary CDF multijet $\not{E}_t$ sample (see text).

One can use data to estimate the background from W and Z decay. A very preliminary estimate of backgrounds is given in Table 1. The heavy quark estimate is from a Monte Carlo study of b production whose normalization cannot be taken seriously until a b cross section is extracted from CDF data. In any case there is no evidence for new physics. In the simple SUSY scenario on which lower limits of 74 and 73 GeV were placed on squarks and gluinos with the 1987 data,[11] even without a background subtraction, a squark limit of about 140 GeV can be obtained. A background subtraction will be needed to obtain a comparable gluino limit.

6. CDF EVENTS WITH LEPTONS

Central electron candidates in CDF are selected by examining the fraction of energy which

Table 1

Preliminary $\not{E}_t$ Events Sources

Process	$\not{E}_t$ > 40 GeV	$\not{E}_t$ > 60 GeV
W → eν	23 ± 14	5 ± 5
W → τν	37 ± 18	---
W → μν	19 ± 9	---
Z → νν	37 ± 18	19 ± 14
$b\bar{b}$ Monte Carlo (normalization?)	42 ± 18	14 ± 5
Sum of the above	158 ± 35	38 ± 17
Data	184	39

The background from various standard physics sources is sufficient to explain the $\not{E}_t$ data.

gets beyond the EM calorimeter ($18X_o$), the transverse energy sharing among scintillator towers, the transverse profiles of the shower measured in the wire/strip proportional chamber at $6X_o$, the position match of the central track to strip chamber coordinates, and the match of energy and momentum. Triggered central muons involve matching the muon drift chamber stub to a good central track in position and slope, and finding appropriate local calorimeter energy. The chambers cover to $|\eta|$ = 0.65. In both cases, cuts on the amount of surrounding energy ("isolation") may be used to reduce jet background. Passive muons were discussed above.

The inclusive electron integral p_T distribution for 2.4 pb^{-1} is shown in Fig. 16. Above 25 GeV/c p_T the spectrum comes essentially from W decay. At lower p_T there is an indication of perhaps 10% background as seen in conversion algorithms, and most of the remainder may be due to b semileptonic decays. To check this hypothesis, Kπ masses are reconstructed for tracks in a $\Delta\eta$, $\Delta\phi$ cone of 1.0 around the electron, looking for the Ds which come from b decay. Simulation, based on the CLEO measurement[12] predict that if the electrons are from b decay 83 ± 19 right sign ($K^\pm$ assignment vs. $e^\pm$) D candidates should be seen. Note that the $K^\pm$ mass is simply assigned, there is no particle ID. As seen in Fig. 17, we observe 62 ± 17 events.
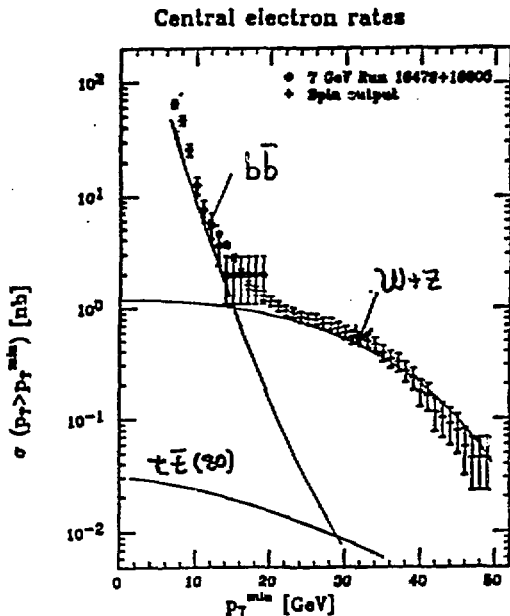

FIGURE 16
Integral electron E_t spectrum for 2.4 pb^{-1} of CDF data (preliminary).

The accurate tracking and well understood central EM calorimeter have been used to extract a measurement of the Z° mass.[13] The data are shown in Fig. 18. As one of muons may be pas-
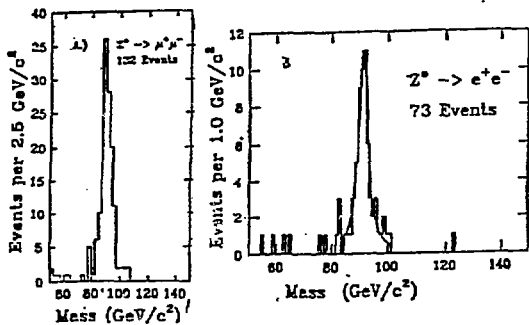

FIGURE 18
Best Z mass sample of a) central muons and b) central electrons from CDF[13].

sive and both electrons must be in good fiducial volume, there are a fewer good electron pairs. The results for muons and electrons are 90.7 = ± 0.4 ± 0.2 GeV and 91.1 ± 0.3 ± 0.4 where the first error is statistical and the second syste-
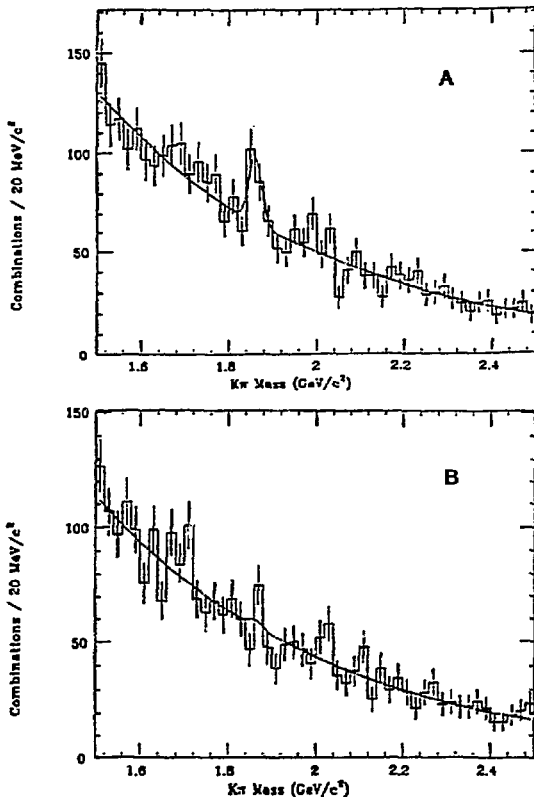

FIGURE 17
Mass distribution for assumed Kπ combinations in a cone around an electron for a) right sign and b) wrong sign combinations from 2.4 pb^{-1} of preliminary CDF data.

matic. These may be combined to give 90.9 ± 0.3 ± 0.2 GeV where the second error is the momentum scale and the first is everything else. While this is a substantial improvement on previous hadron collider measurements, eventual e$^+$e$^-$ measurements will reduce this result to a confirmation of calibration.

It is illuminating to be much less demanding in selecting candidates for Z → ee. A sample of Drell-Yan and Zs has been obtained from diphoton triggers in any EM calorimeter. The resulting spectrum of 597 events is shown in Fig. 19. The low tail is cut off by software threshold and, along with the high tail, is consistent with Z plus Drell-Yan expectation. The overall efficiency is 66% and there are no events above 200
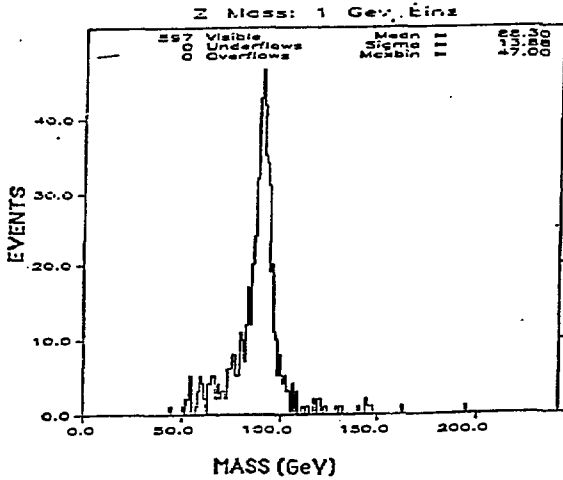
FIGURE 19
Preliminary inclusive CDF Z mass.

GeV. This yields a preliminary 95% CL limit
of $\sigma*B(ee) < 1$ pb for Z' production or $M(Z') >$
400 GeV for standard coupling. Similarly for
Ws, in a slightly less than optimal analysis
there are no events with transverse mass above
150 GeV and with an efficiency for central elec-
trons of about 12%, a preliminary 95% CL limit
of $\sigma*B(ee) < 7.6$ pb corresponds to $M(W') > 380$
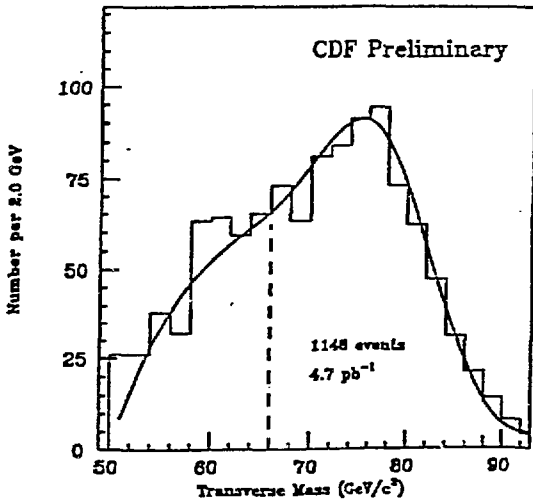GeV for standard coupling.

FIGURE 20
Transverse mass for electron W candidates, E_t
and E_t above 25, no cluster above 7 GeV
(preliminary).

The transverse mass distributions of clean
central electron events, Fig. 20, and central
muon events, Fig. 21, is under intense study to
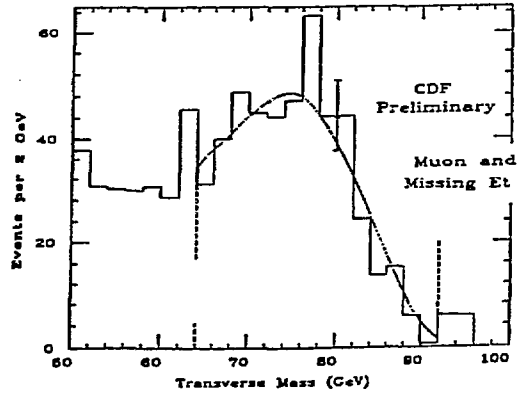determine the W mass. Electron candidates

FIGURE 21
Transverse mass for muon W candidates, E_t and E_t
above 20, no cluster above 7 GeV.

require $E_T(e)$ and E_t above 25 GeV, a good fidu-
cial region electron with E/p < 1.4 and no
cluster above 7 GeV. Muon candidates require E_t
and missing E_t above 20 GeV, isolation, no clus-
ter above 7 GeV and no other track above 15
GeV/c to remove Z and cosmic ray events. The
current fit values are 80.0 ± .2 ± .6 and 79.9 ±
.4 ± .6 for electrons and muons. The errors are
summarized in Table 2. The understanding of
fitting details and resolution unfolding with
$P_t(W)$ are under study and may improve somewhat.
Note that systematic errors in the case of muons
and electrons are generally common.

Note that if one uses electron and muon aver-
ages for the Z and W of 90.9 ± 0.36 and 80.0 ±
0.63 this gives (cancelling common scale) $\sin^2$
θ_w of 0.225 ± 0.013. If one substitutes the
Mark-II Z mass[14] of 91.17 ± 0.17, $\sin^2 \theta_w$
becomes 0.230 ± 0.013. This illustrates that
the calibration scale error which has character-
ized previous hadron collider W and Z mass
measurements[15] is not dominant in the CDF
measurements.

Table 2

Uncertainties in the W Mass (Preliminary MeV)

Source	Electron	Muon
Statistics (Γw free)	200 (380)	430 (440)
Mass Scale	320	160
Radiative Corrections	100	100
Structure Functions	300	300
Resolution p_t (w) etc.	400	400
Background	≤ 50	≤ 200
Fitting Procedure	250	250
Overall Systematic	650	600
Overall	650 (730)	740 (750)

As the analysis becomes less preliminary, the radiative corrections, resolution, and fitting procedures are particularly areas of expected improvement.

Although W and Z production rates have not been extracted from the recent data, there is a preliminary measurement of the production ratio R of W → ev to Z → ee. This ratio is fairly well predicted as a function of the number of light neutrinos and the top mass (in the region where W → t$\bar{b}$ is being closed by phase space). This analysis starts with a common tight good central electron requirement above 20 GeV E_t, and a loose requirement on either E_T for Ws or another electron candidate and 65 < M (e^+e^-) < 115 GeV for Zs. Clean events, with no additional cluster above 10 GeV are used; the preliminary sample yields 204 Z and 1945 W candidates. The number of Zs dominates the error. Relative acceptance is 0.93 ± 0.03 where the error comes from varying structure functions assumed. Efficiencies are thought to be known to ± 2.5%. Cross talk and other background is measured to be 6 ± 1% for Ws and 3.5 ± 2.5% for Zs. This gives R = 10.3 ± 0.8 ± 0.5 where the second error is systematic. The implications are illustrated in Fig. 22. A comparable result has been shown from UA2.[16]
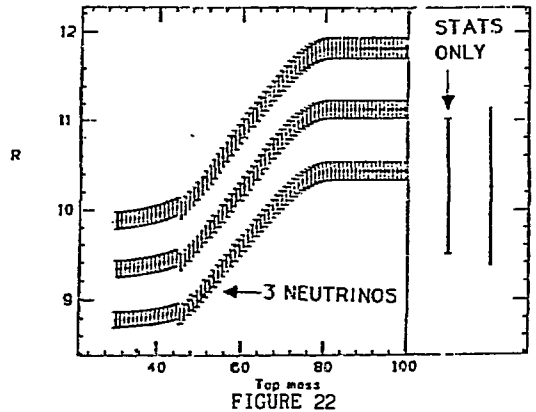

FIGURE 22

Implications of the measurement of σ(W → ev)/σ (Z → ee) for the number of neutrinos and the top mass.

Production of Ws and Zs with accompanying jets should be well described by QCD. The relative rates of accompanying jets for W → e candidates is compared to predictions[17] in Fig. 23. The p_T of Ws and Zs, without smearing corrections, is shown in Fig. 24 and is well described by QCD predictions[18] with at most an event or two extra at very high p_T among the Zs.
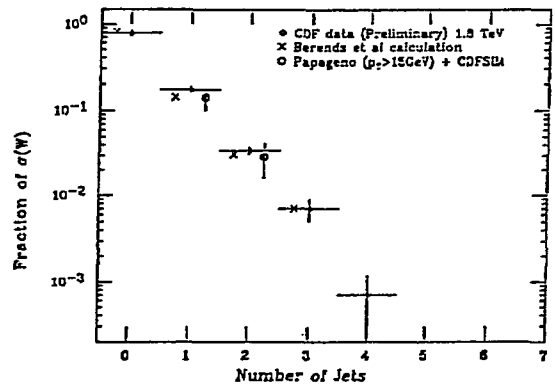

FIGURE 23

Jet counting in CDF W candidates (preliminary). Predictions involve Refs. 7 and 17.

Given that events of the form electron and jets seem to be well interpreted as IVB production, one may ask if there is room in that data for other physics, such as top production with
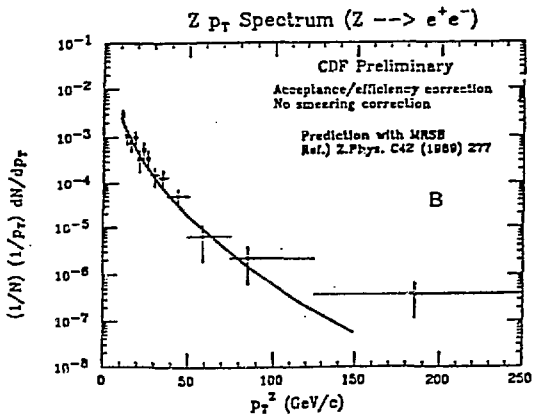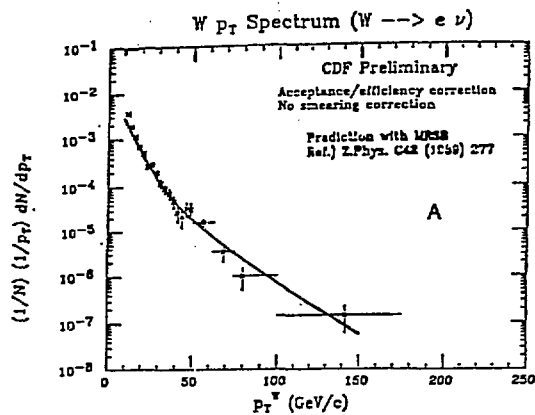
W p_T Spectrum (W --> e ν)

CDF Preliminary

Acceptance/efficiency correction
No smearing correction

Prediction with MRSB
Ref.) Z.Phys. C42 (1959) 277

A

Z p_T Spectrum (Z --> e^+e^-)

CDF Preliminary

Acceptance/efficiency correction
No smearing correction

Prediction with MRSB
Ref.) Z.Phys. C42 (1989) 277

B

FIGURE 24

CDF preliminary p_t distributions (no smearing corrections) for a) W candidates and b) Z candidates. The predictions are from Ref. 18.
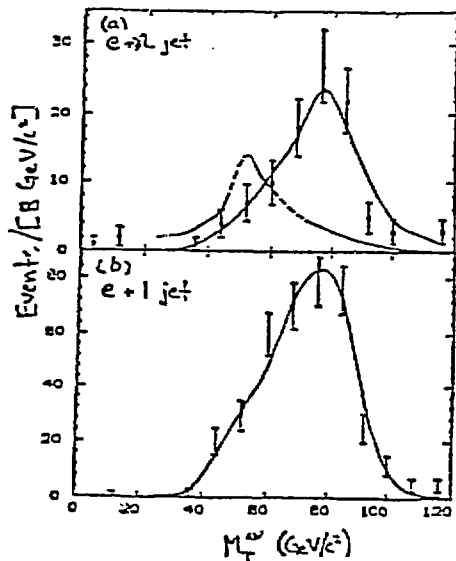

FIGURE 25

Electron-jet top sample transverse mass for events with a) two or more clusters and b) one or more. The data is consistent with W + jets. The effect of a 70 GeV top is illustrated.
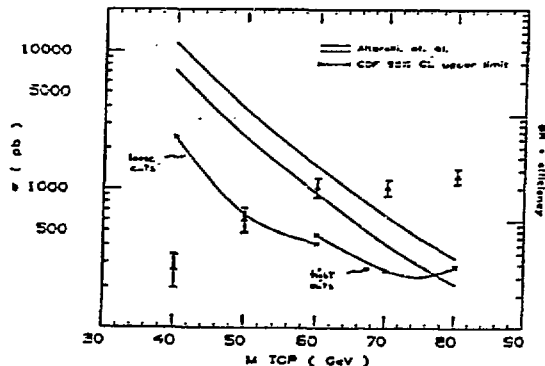

FIGURE 26

CDF top cross section limit from e jet events. The band is the range expected from Ref. 19. Efficiency scale is on the right.

one semileptonic decay. Events with a good central electron and two other clusters above 10 GeV within $|\eta| < 2$ are used in this search. A tight electron isolation requirement is used to reduce background from b decay. Loose and tight cuts on E_T and $E_T(e)$, appropriate for low and high top mass range, are $E_t > 15$, $E_t > 15$, $E_t + E_t > 40$ and $E_t > 20$, $E_t > 20$ (all GeV). A limit on possible top cross section is extracted by fitting the transverse mass distribution (above 24 GeV to avoid QCD and b background) to a linear combination of W plus jets and predicted top signals. This is illustrated in Fig. 25. After folding in systematics, a 95% CL limit is compared to the theoretical range of $t\bar{t}$ cross section[19] in Fig. 26, along with efficiency.

The range of acceptable efficiency and limit less than the low edge of the theoretical range corresponds to $40 > M_T > 77$ at 95% CL. Note that we conservatively ignore $W \to t\bar{b}$.

A relatively clean but less prolific signature for top pairs is to require both to decay semileptonically, in particular to e and μ. Good central electrons above 15 GeV E_t may be
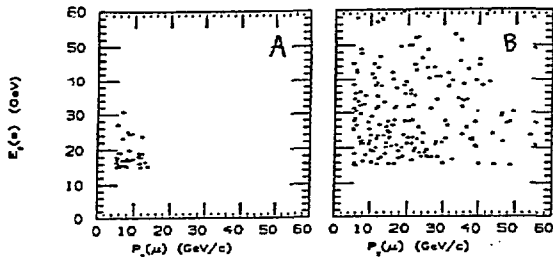
FIGURE 27
Electron and muon E_t for a) 4.6 pb^{-1} of CDF
data and b) 80 pb^{-1} of 70 GeV top Monte Carlo.

accompanied by an opposite sign triggered or
passive muon candidate. The data, along with an
80 pb^{-1} 70 GeV top Monte Carlo prediction are
shown in Fig. 27. The signal region, defined to
be both $E_t(e)$ and $E_t(\mu) > 15$ GeV, contains one
event whose interpretation is ambiguous. Due to
the threshold for lepton transverse energy, the
efficiency drops rapidly below $M_T \approx 30$.
Although predicted backgrounds, notably from
standard model W pair production at 0.15 events,
add to about one event, we define a limit with
no subtraction, systematics folded in, in Fig.
28. The range of comfortable efficiency and
high enough predicted cross section gives 30 >
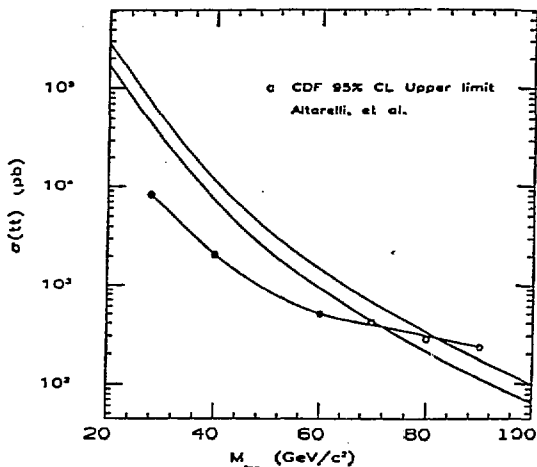$M_T > 72$ GeV at 95% CL. This limit also applies

FIGURE 28
CDF top cross section limit from e + μ events.
The band is expectation from Ref. 19.

to hypothetical fourth generation b' quarks if
they decay promptly by the weak charged current.

7. CDF PHYSICS SUMMARY

Hard scattering in $p\bar{p}$ collisions at 1.8 TeV
involves large and small cross sections for
events with jets or leptons or both which are
reasonably well predicted in the standard model.
Only the usual handful of odd events offer some
sign that some new physics may be lurking just
over the horizon. The study of IVB production
is quite fruitful and in particular, the abso-
lute measurement of the W mass, which is pro-
gressing rather well, may be the most signifi-
cant number from hadron colliders in the near
term.

The continued absence of the top quark is
disappointing, but it is causing various theore-
tical prejudices to be reconsidered. The whole
array of standard model measurements seem to be
compatible with heavy top.[20] There is reason-
able hope for extending the search with existing
data. Beyond that, the $t\bar{t}$ cross section is such
that each factor of two in luminosity can give a
14% improvement in mass reach.

While the CDF collaboration is only just get-
ting started at coming to grips with the new
data, a major boost in luminosity seems needed
to push hard toward the new discovery frontier.
This is in the works.

8. TEVATRON-I OUTLOOK

Various accelerator improvements are in the
works to continue the growth of luminosity. For
the forthcoming run in 1991, most notable among
the antiproton source and Tevatron improvements
is the system of electrostatic separators.
These, by allowing collisions only at B0 and D0,
allow greater intensity and smaller emittance; a
luminosity in excess of 5×10^{30}/cm/sec is anti-
cipated which should yield a sample in excess of
25 pb^{-1}. For the next run, presumably in 1993,

to hypothetical fourth generation b' quarks if they decay promptly by the weak charged current.

7. CDF PHYSICS SUMMARY

Hard scattering in $p\bar{p}$ collisions at 1.8 TeV involves large and small cross sections for events with jets or leptons or both which are reasonably well predicted in the standard model. Only the usual handful of odd events offer some sign that some new physics may be lurking just over the horizon. The study of IVB production is quite fruitful and in particular, the absolute measurement of the W mass, which is progressing rather well, may be the most significant number from hadron colliders in the near term.

The continued absence of the top quark is disappointing, but it is causing various theoretical prejudices to be reconsidered. The whole array of standard model measurements seem to be compatible with heavy top.[20] There is reasonable hope for extending the search with existing data. Beyond that, the $t\bar{t}$ cross section is such that each factor of two in luminosity can give a 14% improvement in mass reach.

While the CDF collaboration is only just getting started at coming to grips with the new data, a major boost in luminosity seems needed to push hard toward the new discovery frontier. This is in the works.

8. TEVATRON-I OUTLOOK

Various accelerator improvements are in the works to continue the growth of luminosity. For the forthcoming run in 1991, most notable among the antiproton source and Tevatron improvements is the system of electrostatic separators. These, by allowing collisions only at B0 and D0, allow greater intensity and smaller emittance; a luminosity in excess of 5×10^{30}/cm/sec is anticipated which should yield a sample in excess of 25 pb^{-1}. For the next run, presumably in 1993,

among other things, the linac upgrade will help emittance, more magnet cooling may allow 2 TeV CM, and an increase in the number of bunches should give greater intensity with fewer events per crossing, while requiring modifications to detector electronics. Luminosity should exceed 10^{31}, integrating to more than 100 pb^{-1} detected. Beyond that there are further antiproton cooling improvements and a major project (the main injector) to remove the main ring from the tunnel to a new smaller one, easing detector backgrounds, giving better emittance matching and allowing test beam running while colliding is in progress. Luminosity should eventually exceed 5×10^{31}.

Upgrades for the CDF detector are also in the works. Various trigger and DAQ upgrades will enable data taking at the higher rates with increased reliability. A four layer 60 μ silicon strip vertex detector is to be installed which should enhance b physics capabilities. New vertex TPCs will have shorter drifts to deal with the higher rates. Central muon coverage will be extended in rapidity and depth, and wire chambers are being added behind the solenoid for direct photon physics. For 1993, new front end electronics, which can deal with the change from 3500 to 400 ns between bunches, is being designed. Options to replace some or all of the gas calorimeters and to effectively close the plug calorimeter from 10 to 2 degrees are being actively pursued. In this case the existing toroids for forward muons can be moved up close to the plug, allowing complete muon coverage. On the other hand, the biggest detector upgrade will be the appearance of a new major detector at D0, shown in Fig. 29.

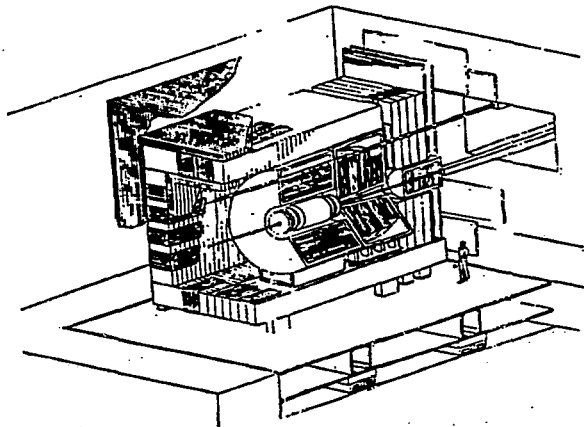part by the U. S. Department of Energy, Division of High Energy Physics, Contract W-31-109-ENG-38.

FIGURE 29
The D0 detector.

REFERENCES

1) R. Rubinstein, (E0) private communication.

2) F. Turkot, Proc. 7th Topical Workshop on Proton Antiproton Physics, Ed. R. Raja, A. Tollestrup, J. Yoh, World Scientific 815 (1989); T. Alexopoulos et al. Phys. Rev. Lett. 60 (1988) 1622; G. Arnison et al. (UA1) Phys. Lett. 118B (1982) 167; G. Piano Mostavi, Proc. Oregon Meeting, Ed. R. C. Hwa, World Scientific 615 (1985).

3) See F. Abe et al. (CDF) , Nucl. Instrum. Meth. A271 (1988) 387 and references therein. Additional material on some of the CDF results covered may be found in A. Garfinkel, H. Grassman, W. Trischuk and R. Hollebeek, these proceedings. Minimum bias results not covered in this report are discussed by M. Binkley, these proceedings.

4) F. Abe et al. (CDF), Phys. Rev. Lett. 62 (1989) 612.

5) E. Eichten, K. Lane, and M. Peskin, Phys. Rev. Lett. 50 (1983) 811.

6) F. Abe et al. (CDF) Phys. Rev. Lett 62 (1989) 3020; F. Abe et al. (CDF) submitted to Phys. Rev. Lett.

7) The α_s^3 event generator provided by I. Hinchcliffe.

8) G. Arnison et al. (UA1), Nucl. Phys. B276 (1986) 253.

9) M. Althoff et al. (TASSO), Z Phys. C22 (1984) 307.

10) UA1 reported on D^* rate of $0.11 \pm 0.05 \pm 0.04$ for $\langle E_t \rangle \approx 43$ GeV, these proceedings.

11) F. Abe et al. (CDF), Phys. Rev. Lett. 62 (1989) 1825.

12) P. Tipton and E. H. Thorndike, CLEO internal report CP-87-26 (unpublished); E. H. Thorndike and R. A. Poling, Phys. Rep. 157 (1988) 183.

13) F. Abe et al. (CDF), Phys. Rev. Lett. 63 (1989) 720.

14) G. S. Abrams et al. (Mark II), Phys. Rev. Lett. 63 (1989) 724.

15) J. M. Gaillard (UA2) presented on W mass $80.0 \pm 0.4 \pm 0.4 \pm 1.2$ GeV and a Z mass $90.2 \pm 0.56 \pm 0.59 \pm 1.4$ GeV, these proceedings.

16) Ibid, ratio at 630 GeV of $10.35 + 1.5 - 1.0 \pm 0.3$ favors heavy top, older measures, C. Albegar et al. (UA1), Phys. Lett. 198B (1987) 271; R. Augari et al. (UA2), Phys. Lett. 194B (1987) 158 favor light top for three neutrinos.

17) F. A. Berends et al., Phys. Lett. B224 (1989) 237.

18) A. P. Martin, R. G. Roberts and W. J. Stirling, Z Phys. C42 (1989) 277.

19) G. Altarelli et al., Nucl. Phys. B308 (1988) 724.

20) R. Barbiari, these proceedings.

DISCLAIMER